Nanocrystalline gold-based hydrogen sulfide (H_2S) sensor from M13 bacteriophage template

Chung Hee Moon[1], Miluo Zhang[2], Nosang V. Myung[2], and Elaine D. Haberer[1,3]

[1]Materials Science and Engineering Program, University of California, Riverside, CA, USA,
[2]Department of Chemical and Environmental Engineering, University of California, Riverside, CA, USA,
[3]Department of Electrical Engineering, University of California, Riverside, CA, USA.

ABSTRACT

Bio-templated assembly enables facile bottom-up assembly of complex and unique nanostructures for chemiresistive gas sensors. Viral-templated gold nanowires have been synthesized for use in highly sensitive H_2S sensors that operate at room temperature. The biological template served as a physical template for gold nanoparticle alignment and as a functional component to enhance sensor sensitivity. Viral-templated gold nanowire H_2S sensors displayed high performance with sensitivity near 850%/ppm, lowest detection limit of 1 ppb, and 70% recovery after 6 min for 0.025 ppm. In comparison, a H_2S sensor in which the viral template was removed showed a 170 times lower sensitivity of 5%/ppm and no recovery. High sensitivity, room temperature operational viral-templated gold nanowire based H_2S sensors have been fabricated and characterized, showing promise of biological-templated nanostructures for enhanced gas sensing.

Keywords: biological template, gold nanowire, M13 bacteriophage, hydrogen sulfide, gas sensor

1 INTRODUCTION

The use of biological molecules is a promising alternative route for synthesis of various nanostructures for electronic applications including chemiresistive gas sensors. The intricate nature of biological molecules allows fabrication of unique nanostructures at ambient temperature and pressure which are not easily obtainable using conventional synthesis methods [1-4]. The high surface-to-volume ratio of such nanostructures enables rapid and efficient interaction of analyte gases with the material surface to improve sensor performance. Hollow spheres of bacteria [1], porous scaffold of pollen grains [2], , and fibrous matrices of eggshells [3] have been used to template solution-based synthesis of ZnO, α-Fe_2O_3, SnO_2, respectively. Such biological-templated hierarchical nanostructures were reported for effective chemiresistive gas sensing at high temperatures after calcination to remove the biological templates [1-3].

Hydrogen sulfide (H_2S) is common industrial hazardous gas released in petroleum, mining, paper, and water treatment industries [5]. Low concentrations of H_2S, below 5 ppm, are harmless, however slightly higher concentrations of 20 ppm, at or above the permissible exposure limit (PEL), can cause eye and respiratory tract irritation. And, exposure to even higher concentrations of 100 ppm, it may cause paralysis and even death [6, 7]. The highly toxic nature and occurrence of H_2S in many industries presents a need for sensitive, low detection limit, low power consuming H_2S gas sensors for continuous environmental monitoring.

In this report, viral-templated chemiresistive H_2S sensors based on gold nanowires are presented. Gold is known for its strong affinity for sulfur-containing compounds such as H_2S and hence, a number of H_2S sensors have been fabricated from various forms of gold nanostructures acting as catalysts or as actual sensing sites [8-12]. A previously reported, genetically-modified gold-binding M13 bacteriophage has been used as the biological template [13]. This filamentous structure that is 880 nm in length and 6 nm in diameter and its specific affinity for gold allow this bacteriophage to be a suitable template for gold nanowire assembly for H_2S sensors. Unlike previous biological-templated H_2S sensors [3, 14], the viral template was not removed prior to gas sensing and was found to play a functional role in enhancing sensor performance by interacting with the H_2S gas. These first sets of experiments demonstrate facile fabrication of sensitive nanostructured gas sensors from biological templates.

2 EXPERIMENTAL DETAILS

2.1 Fabrication of Viral-Templated Gold Nanowire H_2S Sensor

Viral-templated gold nanowire sensors were fabricated on pre-patterned gold electrodes following a procedure adapted from previous reports [15, 16]. Gold electrodes that were 50 μm wide on each side and 3 μm apart were fabricated on Si/SiO_2 substrates using standard optical lithography and microfabrication techniques. A gold-binding M13 bacteriophage [13] with specific affinity for gold was adsorbed onto the substrate by incubating a O_2 plasma-treated substrate in a bacteriophage solution of $3x10^8$ pfu/μL. The substrate was then washed with tris-buffered saline (TBS) with 0.7% Tween 20 and deionized water. Gold nanoparticles (5 nm, BBI Solution) were selectively bound to adsorbed gold-binding phages through

immersion in a gold nanoparticle solution for 1 hr followed by 3 rinses with deionized water and gentle dry with air. These gold nanoparticles were used as seeds for further gold electroless deposition using Nanoprobes GoldEnhance™ LM solutions for 3 min. The final viral-templated devices are hereon referred as "as-assembled" devices. Some of these as-assembled devices were further treated with a short O_2 plasma and ethanol dip which removed the viral template and surface organics, as well as Au_2O_3 which may have been generated by exposure to O_2 plasma [17, 18]. These devices will be referred as "ethanol-treated" devices hereafter.

2.2 Morphological and Electrical Characterization

Scanning electron microscopy (SEM, Phillips XL30 FEG) was used to determine the morphology and spatial distribution of the gold nanowires on the device. Approximately 100 gold nanocrystals were measured to determine the nanoparticle sizes after gold electroless deposition. The room temperature resistances of viral-templated gold nanowire devices were determined using two-terminal, current-voltage (I-V) measurements in which the current was recorded as the applied voltage was swept from -0.3 V to 0.3 V (Keithley 2636A sourcemeter).

2.3 Sensing Analysis

Selected viral-templated gold nanowire devices were wire-bonded (West-bond Inc. 7499D) to a copper printed circuit board with 1% Si/Al wire for sensing analysis. Sensing analysis was performed under ambient temperature and pressure. Sensors were placed in a closed chamber with gas inlet and outlet. The resistance change of the viral-templated devices was measured while applying a constant bias of 0.15 V and flowing different H_2S gas concentrations ranging from 0.025 ppm to 40 ppm. Dry air was used as the carrier gas, as well as to dilute the analyte gas to the desired concentration. A mass flow controller with LabView interface was used to control the H_2S concentration and exposure time.

3 RESULT DISCUSSION

3.1 Morphological and Electrical Analysis

The morphology and areal distribution of viral-templated gold nanowires assembled on the H_2S sensors were observed using SEM. Figure 1(a) shows representative low and high magnification images of viral-templated gold nanowires across the 3 μm gap within the sensor. The gold nanowires that are slightly less than 1 micron in length and composed of well-defined nanoparticles in a chain-like form were randomly distributed on the substrate. As shown in the high magnification SEM image in figure 1(b), the width and connectivity varied along individual nanowires, as well as from nanowire to nanowire. Further SEM analysis revealed that the number of gold nanoparticle seeds per template ranged from 31 to 61 with an average of 42. This large distribution suggested that the deviations in nanowire width and connectivity were greatly affected by the differences in the density and arrangement of gold nanoparticle seeds on the gold-binding phage prior to electroless gold deposition. The nanoparticles within the nanowires were polydisperse with an average width of 29±7 nm. The assembled gold nanowires formed a continuous, mesh-like structure between the electrodes. Given the relative size of the gold nanowires and electrode gap, multiple nanowires were required to physically bridge the gap between the two electrodes. No difference in the morphology, structural dimensions, or distribution of nanowires on the device was observed with SEM after template removal by O_2 plasma and ethanol treatment.

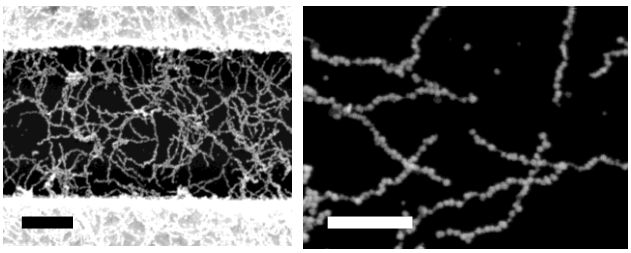

Figure 1. (a) Low magnification SEM image to show nanowire density and distribution within the 3 μm gap of the device. Scale bar is 1 μm. (b) High magnification SEM image of gold nanowires to show morphology and nanocrystal arrangement. Scale bar is 500 nm.

The electrical resistances of the viral-templated devices were measured from -0.3 V and 0.3 V range at room temperature. All measured devices displayed Ohmic behavior but the device-to-device resistance varied by 1 to 4 orders of magnitude with most as-assembled devices showing 10^8 to 10^9 Ω resistance. Similar to morphological deviations, the large resistance distribution of the devices is attributed to the differences in gold seed nanoparticle density and arrange on the template. To better understand the impact of the phage template and surface organics on sensor resistance, two-terminal measurements were also performed on ethanol-treated devices. Resistance of ethanol-treated devices also showed large distribution, but the resistances decreased significantly with most ethanol-treated devices showing 10 to 100 Ω resistance. Nonconductive organic ligands act as energy barriers to charge transport via electron hopping in metal nanoparticle films and chains, often resulting in highly resistive materials [19-21]. The large decrease in resistance observed in ethanol-treated sensors was attributed to the removal of organic components such as peptides and viral template from gold nanoparticle surfaces resulting in reduced nanoparticle-to-nanoparticle energy barriers and enhanced charge transport [21-23].

3.2 Sensing Analysis for H_2S

Representative real-time sensing behaviors of as-assembled and ethanol-treated viral-templated gold nanowire sensors are shown in figures 2(a) and (b). For each device, the change in resistance relative to the baseline resistance ($\Delta R/R_0$) is shown as a function of time. A stable resistance baseline was established for each device after exposure to dry air flow for 5 hr while applying a constant bias. Both the as-assembled and ethanol-treated viral-templated devices showed an increase in resistance with each exposure to H_2S gas analyte. The resistance increase was consistent with other reports of H_2S sensors composed of gold NP chains [10, 11, 24] and films [25] in which charge transport between neighboring nanoparticles or nanocrystals was impeded by adsorption of H_2S on the gold surface.

Apart from the resistance increase with each H_2S exposure, the as-assembled devices and ethanol-treated devices, with and without phage respectively, displayed very different sensing behaviors at the same analyte concentration range. The as-assembled device in figure 2 (a) showed rapid initial response rate to H_2S exposure that decreased with longer exposure times. Within the 0 to 0.025 ppm linear range the sensitivity was 846%/ppm, which is more than an order of magnitude greater than other gold-based room temperature H_2S sensors [8, 11, 25]. Saturation was observed at concentrations above 0.025 ppm. The

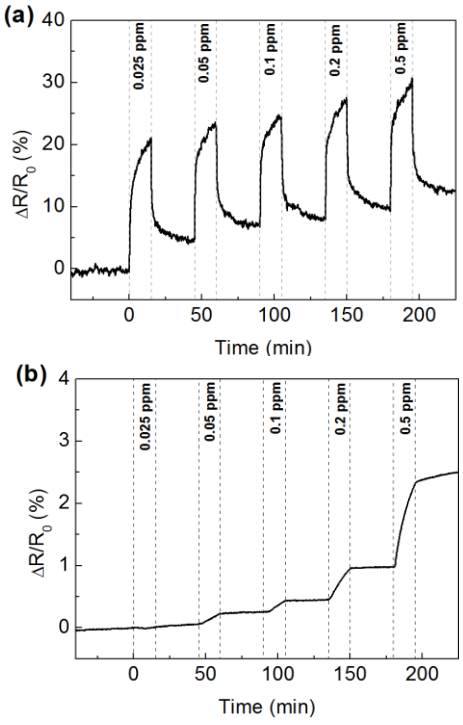

Figure 2. Representative real-time sensing behaviors (a) as-assembled and (b) ethanol-treated viral-templated device. H_2S gas and dry air introduced to sensing chamber at intervals of 15 min and 30 min, respectively. The H_2S gas concentration for each exposure as indicated.

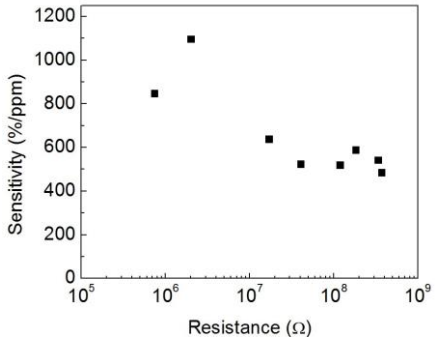

Figure 3. Dependence of sensor sensitivity on electrical resistance in the as-assembled devices.

lowest detection limit, defined as the concentration at which the response is 3 times the signal-to-noise ratio, was 1 ppb. This value is lower than that achieved by H_2S sensors composed of electrophoretically-assembled glycine-stabilized gold nanoparticles [11] and gold nanoparticles on 1-pyrenesulfonic acid-coated carbon nanotube templates [10], and comparable to the 3 ppb limit reported for sensors assembled from carbon nanotubes decorated with electrochemically deposited gold [8]. The response and recovery times were greater than 15 min and 30 min, respectively. Seventy percent recovery was observed within 30 min for all as-assembled devices, indicating desorption of the gas analytes from the surface. Faster recovery was observed with exposure to lower analyte concentrations where devices exposed to 0.025 ppm H_2S displayed 70% recovery within 6 min. The sensitivity dependence on device resistance is shown in figure 3. Sensitivity generally decreased with increased device resistance. Further studies need to be completed to fully understand the nature of this behavior.

In comparison, the ethanol-treated devices, without the biological template present, displayed a slower response time, increasing in resistance throughout the entire 15 min H_2S exposure as shown in figure 2 (b). These devices displayed sensitivity of 5%/ppm and lowest detection limit of 5 ppb. Unlike the as-assembled devices, no recovery was observed in the ethanol-treated sensors. This irreversible behavior suggests the continued presence of analyte or analyte products on the gold nanowire sensor surface. This is consistent with findings for other gold-based H_2S sensors at room temperature in which recovery was only observed at temperatures greater than 140°C due to strong Au-S affinity [10, 24, 25].

The sensing performance of the as-assembled sensors was superior to the ethanol-treated sensors exhibiting a lower detection limit, significantly increased sensitivity, and decreased response and recovery times. This suggests the possibility that the viral-template has an active role, in addition to its primary role as a physical template, in device-analyte interaction. Further studies need to be completed to better understand the role of the viral-template and gold-binding peptide in sensor performance, as well as adsorption and desorption kinetics.

4 CONCLUSION

This report presents a simple biological template-based method for fabrication of highly sensitive gold H_2S sensors at room temperature. The viral-templated gold nanowires, composed of chains of nanocrystals, connected the device electrodes in a mesh-like form enabling electrical conduction. The electrical resistances of the devices showed a wide distribution with most devices in 10^8 to10^9 Ω range. The as-assembled devices showed superior sensor performance with sensitivity of about 850%/ppm, lowest detection limit of 1 ppb, and 70% recovery after 6 min for 0.025 ppm. The removal of the viral-template had a significant effect on the device behavior, decreasing the resistance to the 10 to100 Ω range and the sensitivity to 5%/ppm. Although further study is needed, these finding suggest a functional role of the viral template and demonstrate the promise of a viral-templated assembly route for effective and improved gas sensor performance.

ACKNOWLEDGEMENTS

The authors will like to thank E. L. Hu (Harvard University) and A. M. Belcher (MIT) for the gift of the gold-binding phage (p8#9). We thank Myung Group members Heng Chia (Charles) Su and Nicha Chartuprayoon for their assistance with the gas sensing system. These studies made use of the Central Facility for Advanced Microscopy and Microanalysis (CFAMM) and Center for Nanoscale Science and Engineering (CNSE).

REFERENCE

[1] Zhang H, Xu C, Sheng P, Chen Y, Yu L and Li Q 2013 *Sens. Actuators B-Chem.* **181** 99-103
[2] Yang F, Su H, Zhu Y, Chen J, Lau W M and Zhang D 2013 *Scripta Materialia* **68** 873-6
[3] Dong Q, Su H, Zhang D and Zhang F 2006 *Nanotechnology* **17** 3968-72
[4] Bruckman M A, Liu J, Koley G, Li Y, Benicewicz B, Niu Z and Wang Q 2010 *J. Mater. Chem.* **20** 5715-9
[5] U.S. Department of Health and Human Services-Public Health Service (Agency for Toxic Substances and Disease Registry) 2006 http://www.atsdr.cdc.gov/toxprofiles/index.asp
[6] Occupational Safety and Health Administration (OHSA) 2005 https://www.osha.gov/pls/publications/publication.html
[7] Pandey S K, Kim K-H and Tang K-T 2012 *Trac-Trends in Analyt. Chem.* **32** 87-99
[8] Mubeen S, Zhang T, Chartuprayoon N, Rheem Y, Mulchandani A, Myung N V and Deshusses M A 2010 *Anal. Chem.* **82** 250-7
[9] Shirsat M D, Bangar M A, Deshusses M A, Myung N V and Mulchandani A 2009 *Appl. Phys. Lett.* **94** 083502
[10] Ding M, Sorescu D C, Kotchey G P and Star A 2012 *J. Am. Chem. Soc.* **134** 3472-9
[11] Lee J, Mubeen S, Hangarter C M, Mulchandani A, Chen W and Myung N V 2011 *Electroanalysis* **23** 2623-8
[12] Geng J F, Thomas M D R, Shephard D S and Johnson B F G 2005 *Chem. Comm.* 1895-7
[13] Huang Y, Chiang C Y, Lee S K, Gao Y, Hu E L, De Yoreo J and Belcher A M 2005 *Nano Lett.* **5** 1429-34
[14] Liu Z, Fan T, Zhang D, Gong X and Xu J 2009 *Sens. Actuators B-Chem.* **136** 499-509
[15] Haberer E D, Joo J H, Hodelin J F and Hu E L 2009 *Nanotechnology* **20** 4215206
[16] Joo J H, Hodelin J F, Hu E L and Haberer E D 2012 *Mater. Lett.* **89** 347-50
[17] Ishida T, Tsuneda S, Nishida N, Hara M, Sasabe H and Knoll W 1997 *Langmuir* **13** 4638-43
[18] Tsai H C, Hu E, Perng K, Chen M K, Wu J C and Chang Y S 2003 *Surface Science* **537** L447-L50
[19] Park S J, Lazarides A A, Mirkin C A, Brazis P W, Kannewurf C R and Letsinger R L 2000 *Angew. Chem. Int. Ed.* **39** 3845-8
[20] Brust M, Bethell D, Kiely C J and Schiffrin D J 1998 *Langmuir* **14** 5425-9
[21] Fishelson N, Shkrob I, Lev O, Gun J and Modestov A D 2001 *Langmuir* **17** 403-12
[22] French R W, Milsom E V, Moskalenko A V, Gordeev S N and Marken F 2008 *Sens. Actuator B-Chem.* **129** 947-52
[23] Sugden M W, Richardson T H and Leggett G 2010 *Langmuir* **26** 4331-8
[24] Geng J F, Thomas M D R, Shephard D S and Johnson B F G 2005 *Chem. Comm.* 1895-7
[25] Yoo K S, Sorensen L W and Glaunsinger W S 1994 *J. Vac. Sci. Techol. A* **12** 192-8